Bioorganic & Medicinal Chemistry Letters 21 (2011) 5274–5282

Contents lists available at ScienceDirect

Bioorganic & Medicinal Chemistry Letters

journal homepage: www.elsevier.com/locate/bmcl

Identification of a series of 4-[3-(quinolin-2-yl)-1,2,4-oxadiazol-5-yl]piperazinyl ureas as potent smoothened antagonist hedgehog pathway inhibitors

Jesus M. Ontoria [a], Laura Llauger Bufi [a], Caterina Torrisi [a], Alberto Bresciani [a], Claudia Giomini [a], Michael Rowley [a], Sergio Serafini [a], Hu Bin [b], Wu Hao [b], Christian Steinkühler [a], Philip Jones [a,*]

[a] IRBM, Merck Research Laboratories Rome, Via Pontina km 30,600, Pomezia, 00040 Rome, Italy
[b] WuXi AppTec Co., Ltd, 288 Fute Zhong Road, Waigaoqiao Free Trade Zone, Shanghai 200131, PR China

ARTICLE INFO

Article history:
Received 18 June 2011
Revised 29 June 2011
Accepted 6 July 2011
Available online 14 July 2011

Keywords:
Hedgehog pathway
Smoothened antagonist
Hedgehog inhibitor

ABSTRACT

The Hedgehog (Hh-) signalling pathway is a key developmental pathway and there is a growing body of evidence showing that this pathway is aberrantly reactivated in a number of human tumors. Novel agents capable of inhibiting this pathway are sought, and an entirely novel series of smoothened (Smo) antagonists capable of inhibiting the pathway have been identified through uHTS screening. Extensive exploration of the scaffold identified the key functionalities necessary for potency, enabling potent nanomolar Smo antagonists like **91** and **94** to be developed. Optimization resulted in the most advanced compounds displaying low serum shift, clean off-targets profile, and moderate clearance in both rats and dogs. These compounds are valuable tools with which to probe the biology of the Hh-pathway.

Several developmental pathways regulate patterning, growth and cell migration during embryonic development, of which the hedgehog (Hh-) signalling pathway is a one of these. While this pathway is critical during development, its role in later life is limited to a small number of tissues and to a maintenance/repair role.[1–4] However, in the last decade evidence has emerged showing that this pathway is aberrantly activated in a growing number of cancers, and strategies to inhibit this pathway are being evaluated for therapeutic use to target defined tumors dependent on this pathway.

The Hh-signalling cascade is initiated by binding of Hh-protein to its cellular membrane receptor Patched (Ptch), and this binding relieves Ptch-mediated repression of the GPCR-like receptor Smoothened (Smo). Alleviation of this repression initiates an intracellular signalling cascade culminating with the Gli-transcription factors (Gli1-3) regulating genes involved in differentiation, proliferation and survival. In tumors, mutations in Ptch and Smo, as well as downstream factors SUFU and Gli, have been identified, thereby activating the pathway.[1,2]

Several agents have been demonstrated to show preclinical antitumor activity in animal models,[3,5] The majority of the research has focused on Smo antagonists, including the natural product Cyclopamine (**1**) (Fig. 1), and various synthetic molecules. Recently, the most advanced of these, Vismodegib (GDC-0449) (**2**),[6] has demonstrated encouraging results in phase I studies in advanced basal cell carcinoma.[7] We have recently disclosed the identification and optimization of a novel series of [6,5]-bicyclic tetrahydroimidazo[1,5-*a*]pyrazine-1,3(2*H*,5*H*)-dione Smo antagonists,[8] culminating in the development of MK-5710 (**3**).[9] An alternative method to inhibit the pathway include small molecule that binds Hedgehog,[10] such as robotnikinin (**4**) as well as binders to Gli proteins like GANT61 (**5**),[11] and other compounds whose mechanisms of action are being elucidated.[12,13]

Herein we described the development of an alternative class of structurally distinct, potent Smo antagonists with acceptable pharmacokinetics in preclinical species, culminating in the identification of **91** and **94**.

The program began with an high throughput screening campaign against the corporate screening collection to identify small molecules useful for the treatment of Hh dependent malignancies where compounds were screened for their ability to inhibit the Hh pathway in Shh-light2 cells expressing a Gli-dependent reporter gene, simultaneously monitoring for cytotoxicity.[14] Hits were then profiled in a whole cell Smo binding assay in 2% fetal bovine serum (FBS), measuring the ability of compounds to displace a Bodipy-labeled cyclopamine derivative.[15] The initial screen identified three closely related 4-[3-(quinolin-2-yl)-1,2,4-oxadiazol-5-yl]piperidinyl urea (**6–8**) as Smo antagonists, and inhibitors of the Hh-pathway (Fig. 2). All three compounds inhibited the pathway with several hundred nanomolar activity, and inhibited binding of the labeled cyclopamine derivative at similar concentrations.

The *ortho*-chloro derivative (**6**) was profiled more extensively and the compound showed high clearance in rat microsomes

* Corresponding author. Present Address: Belfer Institute for Applied Cancer Sciences, Dana Farber Cancer Institute, 450 Brookline Avenue, Boston, MA 02115, USA. Tel.: +1 617 582 9648.
E-mail address: philip_jones@dfci.harvard.edu (P. Jones).

0960-894X/$ - see front matter © 2011 Elsevier Ltd. All rights reserved.
doi:10.1016/j.bmcl.2011.07.031

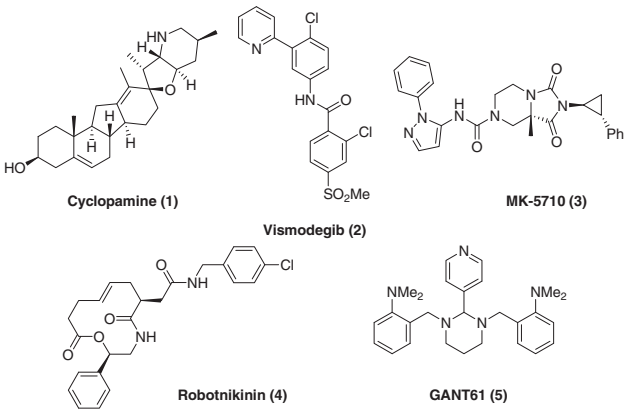

Figure 1. Representation Hh-pathway inhibitors.

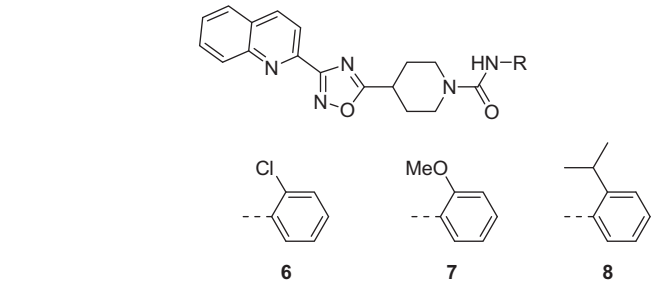

Light2 IC_{50} (nM)	510	410	480
Smo Bind 2% FBS IC_{50} (nM)	380	180	350

Figure 2. Lead structures from uHTS campaign.

(Cl_{int} >200 μL/min/mgP) and moderate clearance in dog and human microsomes (Cl_{int} = 65 and 45 μL/min/mgP respectively). In vivo the compound showed low clearance in rats with Cl = 11 min/ml/kg, which could be attributed to the lipophilic nature of the compound which displayed log *D* = 4.25, and high plasma protein binding (fraction unbound (f_u) rat 1%, human 0.5%). The oral bioavailability of **6** was acceptable at 38%. Limited metabolite identification studies in microsomes pointed towards the piperidine and chlorophenyl groups as being prone to oxidative metabolism. The compound displayed some off-target activity with modest hERG activity (62% inh. at 10 μM), and also inhibition of CYPs 2C9 and 3A4 (62 / 58% inh. at 10 μM).

Encouraged by these results, further SAR exploration was undertaken, extensively exploring the SAR of each of the four components of the lead scaffold: the quinoline ring system; the 1,2,4-oxadiazole; the piperidine ring system, and the right hand side capping group.

Initial studies exploring the importance of the 1,2,4-oxadiazole rapidly established that this isomeric ring system was critical from binding to Smo, as the alternative isomers (**9** and **10**) were inferior to **7** (Table 1). The isomeric 1,2,4-oxadiazole (**10**) was round 6-fold less active, while the corresponding 1,3,4-isomer (**9**) displayed only weak micromolar affinity.

Similar studies were conducted to explore the importance of the piperidine ring (Table 2), and ring contraction to either the corresponding azetidine or pyrrolidine ring systems resulted in abolishment of affinity for Smo, with both **11** and **12** showing only modest inhibition at 10 μM.

Knowing that the piperidine moiety of **6** was one of the sites for oxidative metabolism, some efforts were undertaken to try and

Table 1
Exploration of the oxadiazole ring system

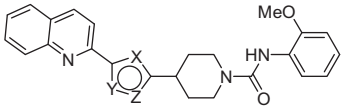

R	Compound	Light2 IC_{50} (nM)[a]	SmoBind 2% FBS IC_{50}(nM)[a]
	**7**	410	180
	**9**	57% inh. at 20 μM	4700
	**10**	2400	15000

[a] Values are means of at least 3 experiments (std. dev. were within 25% of the IC_{50} values).

Table 2
Exploration of the central saturated heterocyclic ring system

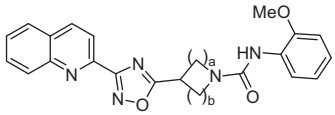

R	Compound	Light2 IC_{50} (nM)	SmoBind 2% FBS IC_{50} (nM)
	7	410	180
	11	28% inh. at 10 μM	39% inh. at 10 μM
	12	15% inh. at 10 μM	38% inh. at 10 μM

Table 3
Effect of substituents on piperidine ring system

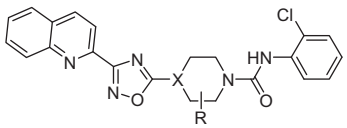

	Compound	Light2 IC_{50} (nM)	SmoBind 2% FBS IC_{50} (nM)
	**6**	510	380
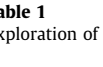	**13**[a]	680	790
	14	900	640
	15	2400	620
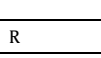	**16**	2500	6000
	17	1300	2100
	18	1300	1000
	19	140	170

[a] Mixture of diastereomers.

prevent this metabolism (Table 3), either by addition of additional substituents, or through changing the electronic of the ring system. Unfortunately, introduction of additional substituents on this 6-membered ring proved to be detrimental to affinity, as all substitute piperidines displayed inferior potency to **6**, even addition of a 4-fluoro group in **18** resulted in a 3-fold loss in activity. However, replacement of the piperidine for a piperazine as in the case of **19**, resulted in a 3-fold improvement in both Smo binding affinity (IC_{50} = 170 nM) and also a similar improvement in activity in the light2 assay, where **19** inhibited the hedgehog pathway with IC_{50} = 140 nM. Noticeably, the introduction of the additional nitrogen in the piperazine scaffold, resulted in lower log *D* = 2.95, and accordingly improved both the CYP inhibition (2D6, 2C9 and 3A4 IC_{50} >25 μM) and hERG (IC_{50} = 12 μM) profiles.

Having established that the central portion of these Smo antagonists was critical for the affinity, attention focused on the two extremities of the molecule, focusing first on replacement of the 2-quinoline ring (Table 4). The bicyclic heterocyclic framework is

Table 4
Exploring the SAR of the left-hand side heterocyclic group

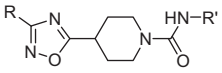

R'	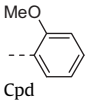		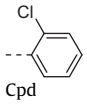	
R	Cpd	SmoBind 2% FBS IC_{50} (nM)	Cpd	SmoBind 2% FBS IC_{50} (nM)
	**20**	>2.5 μM	**21**	>2.5 μM
	**22**	>2.5 μM		
	**23**	>2.5 μM	**24**	>2.5 μM
	**25**	>2.5 μM	**26**	>2.5 μM
	**27**	>2.5 μM		
	**28**	51% inh at 2 μM	**29**	63% inh at 2.5 μM
	**30**	>2.5 μM	**31**	>2.5 μM
	**32**	>2.5 μM	**33**	>2.5 μM
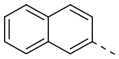	**34**	2200		
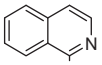	**35**	>2.5 μM	**36**	>2.5 μM
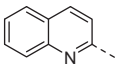	**7**	180	**6**	380
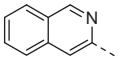	**37**	750		
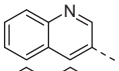	**38**	1900	**39**	>2.5 μM
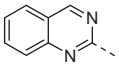			**40**	>2.5 μM
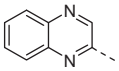			**41**	1100
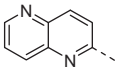			**42**	>2.5 μM
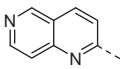			**43**	2200
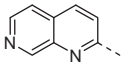			**44**	>2.5 μM
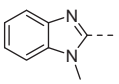			**45**	1000

important for potent inhibition of the hedgehog pathway, as alteration to a simple phenyl (**20–21**), or monocyclic heterocycle such as pyridines (**23–27**), pyrimidine (**30–31**) or pyrazine (**32–33**) resulted in significant losses in activity. Only the addition of a 3-methyl-2-pyridyl group in **28** resulted in some modest inhibition of the pathway with around 50% inhibition at 2 μM. When the 2-quinoline was replaced by a 2-naphthyl group approximately a 10-fold loss in potency was observed with **34** displaying IC_{50} = 2.2 μM. This position of the nitrogen in the quinoline ring was critical as when the corresponding 1-isoquinoline (**35–36**), or 3-isoquinoline were prepared these too displayed inferior inhibition of the Hh-pathway with **37** displaying IC_{50} = 0.5 μM in the Smo binding assay and IC_{50} = 1.6 μM in the light2 assay. Similarly the 3-quinoline **38** display IC_{50} = 1.9 μM in the binding assay. Addition of a second nitrogen into the bicyclic scaffold also proved to be detrimental as quinazoline (**40**), quinoxaline (**41**), and naphthyridines (**42–44**) all showed weaker activity than the corresponding 2-quinoline (**6**), with the quinoxaline (**41**) being the most potent of these displaying IC_{50} = 1.1 μM in the Smo binding assay. In contrast, one suitable replacement for the 2-quinoline group proved to be the corresponding *N*-methylbenzimidazole, and while **45** displayed slightly weaker affinity in the binding assay with IC_{50} = 1.0 μM, it appeared to be equipotent with **6** in the light2 assay (IC_{50} = 430 nM). Interestingly this more polar compound, measured log *D* = 2.85, proved to have improved hERG profile (IC_{50} = 32 μM), and reduced CYP inhibition liabilities (2C9: 44% inh., 3A4: 35% inh. at 10 μM).

Knowing that the 4-[3-(quinolin-2-yl)-1,2,4-oxadiazol-5-yl]piperidinyl ring system was one of the best core scaffolds with which to interrogate the left hand side SAR, attention focused on the urea fragment (**Table 5**). It was rapidly established that aromatic ureas were one of the best functionalities to introduce at that position as simple amides were generally inactive, and only when large lipophilic moieties like the cycloheptane group (**46**) were introduced was good inhibition of the Hh-pathway seen. Similarly alkyl groups such as cyclohexylmethyl (**47**) or *ortho*-chlorobenzyl (**48**) displayed only micromolar activity. The corresponding carbamate analogy **50** was demonstrated to be equipotent to **7**, however, during further study it was shown that the phenolic carbamates were unstable and rapidly cleaved. The homologated benzyl carbamate (**51**) was displayed weaker micromolar activity. With this knowledge an in-depth study into the urea group was conducted, where it was rapidly established that an aromatic urea was beneficial for activity as the ethyl urea (**52**) was displayed greater than 2.5 μM activity in the Smo binding assay, whereas a simple phenyl urea (**53**) displayed IC_{50} = 480 nM. It was also established that primary ureas were preferred over secondary ureas, as methylation of the NH of **7** to give **56** resulted in a 8-fold loss in activity (Smo bind IC_{50} = 180 vs. 1400 nM), similarly when the tolyl derivative **57** was cyclised to the corresponding tetrahydroquinoline urea (**58**) a substantial loss in activity was observed in the functional assay (Light2 IC_{50} = 440 vs. 2300 nM).

Substituents were tolerated on the aniline ring at the *ortho*- and *meta*- positions, although introduction of a *para*-methoxy (**55**) group resulted in a loss of activity (68% inh at 4 μM). A wide range of substituents could be accommodated at the *ortho*-position without having a significant impact on the affinity of these Smo antagonists, including methoxy (**7**), chloro (**6**), methyl (**57**), trifluoromethyl (**60**), isopropyl (**8**) and nitrile (**61**) groups. However, formation of a ring between the *ortho* and *meta*-positions, as in quinoline (**62**) was found to cause around a 3-fold loss in affinity. Similarly introduction of heteroatoms into the aromatic ring proved to be detrimental as the corresponding pyridine derivatives of **6**, compounds **63–65**, all displayed between 3- and 6-fold weaker affinity than the chloroaniline, and similarly the isoxazole (**66**) displayed only micromolar affinity.

When larger more lipophilic alkyl ureas were explored an interesting trend was observed, and cycloalkyl ureas like cyclopentyl (**68**) and cyclohexyl (**69**) displayed sub-micromolar activity in both assays. In particular, the cyclohexyl **69** had a very interesting profile, inhibiting the pathway with IC_{50} = 57 nM in the light2 assay and showing IC_{50} = 280 nM in the binding assay, where it competes for binding against Bodipy-cyclopamine. Despite the increase in potency of this compound, the cyclohexyl urea suffered from both high turnover in rat microsomes (Cl_{int} >300 μL/min/mgP) and high plasma protein binding (human f_u = 0.5%). The corresponding carbamate (**70**) was round 10-fold less active in the functional assay, with IC_{50} = 580 nM.

Having established the initial SAR in this series, attention focused on optimizing the best compounds from this series, and attention focused on some specific areas. Most notable was the potency of these compounds, and the majority of these compounds still displayed activities in the hundreds of nanomolar range, with **69** being one of the most active compounds, light2 IC_{50} = 57 nM. Secondly, the high lipophilicity of these compounds needed to be addressed as these Smo antagonists displayed high plasma protein binding and serum shift. Accordingly, the binding assay was optimised so that compounds could also be evaluated in the presence of 20% normal human serum (NHS). For example, when **6** was tested in the Smo binding assay in the presence of 20% NHS, the IC_{50} shifted about 10-fold, IC_{50} = 3.5 μM. Initial data suggested this could be improved by modulating the log *D* of these compounds as the corresponding *N*-methylbenzimidazole (**45**) with measured log *D* = 2.85, proved to have a reduced serum shift, with only a 5-fold loss in activity when the binding assay was run in the presence of 20% NHS (IC_{50} = 1.0 and 4.5 μM respectively). Similarly, the piperazine bearing the *ortho*-chloroaniline (**19**) displayed only a 4-fold shift in the Smo binding assay, displaying with IC_{50} = 170 and 700 nM in the presence of 2% FBS and 20% NHS respectively. The third area for improvement was the stability of these compounds in liver microsomes, as the majority of these compounds displayed high turnover in rat liver microsomes **6**: Cl_{int} >200, benzimidazole (**45**): = 174, and cyclohexyl (**69**): >300 μL/min/mgP.

Attempts to reduce the plasma protein binding of lead **6** focused on the introduction of polar substituents on either the left- or right-hand side of the leads structures, as demonstrated from the previous work that neither the quinoline or phenyl groups could be altered to more polar heterocycles. Addition of a polar nitrile, or methylsulfone on the urea fragment generally resulted in a loss of potency (**Table 6**), however, the introduction of the *para*-methylsulfone in **71** did result in result in a reduction of serum shift to only 3-fold, with Smo Bind IC_{50} = 1.5 and 4.1 μM respectively and log *D* = 2.8. Alternatively, addition of a methoxy group at various positions of the quinoline was also attempted, and resulted in a substantial loss of activity (similar results were seen with other substituents, data not shown). The exception to this was the introduction of groups at the 5- or 6-position, which was tolerated to a limited extent, although frequently resulting in a 5-fold loss in potency.

Attention then switched to the cyclohexyl urea moiety in an effort to address primarily potency and stability, and to a lesser extent the serum shift (**Table 7**). Initial data revealed that the introduction of polar functionality in this region of the molecule was detrimental for affinity, as the introduction of a hydroxyl group (**81**), or alteration of the cyclohexyl to either a pyran (**82**) or a functionalised piperidine (**83–85**) resulted in a loss in potency. Interestingly, both the piperidine (**83**) and the *N*-acetyl piperidine (**85**) display minimal serum shift. A significant breakthrough came with the discover of the thiopyran dioxide (**87**) and 4,4'-difluorocyclohexyl (**88**) derivatives, for although these two compounds showed inferior activity to **69**, they both displayed

Table 5
Exploring the SAR of the right-hand side urea and related groups

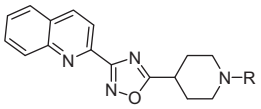

R	Compound	Light2 IC_{50} (nM)	SmoBind 2% FBS IC_{50} (nM)
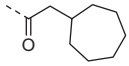	**46**	840	1000
	**47**		>2.5 μM
	**48**		>2.5 μM
	**49**		>2.5 μM
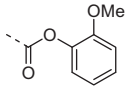	**50**	250	110
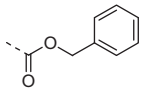	**51**	>2.5 μM	>2.5 μM
	**52**		>2.5 μM
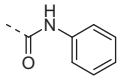	**53**		480
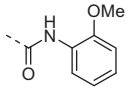	**7**	410	180
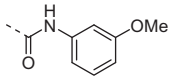	**54**	410	220
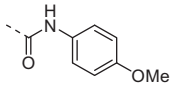	**55**		>2.5 μM
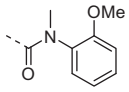	**56**	3100	1400
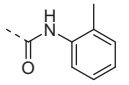	**57**	440	510
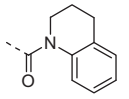	**58**	2300	670
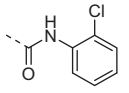	**6**	510	380
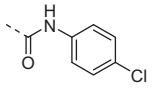	**59**		470
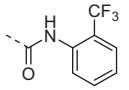	**60**	700	340
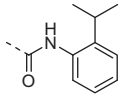	**8**	480	350

Table 5 (*continued*)

R	Compound	Light2 IC_{50} (nM)	SmoBind 2% FBS IC_{50} (nM)
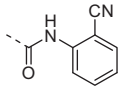	**61**	190	490
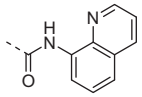	**62**	1400	1300
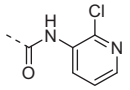	**63**	1600	1500
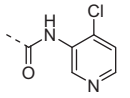	**64**	2000	1100
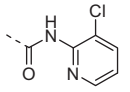	**65**	2800	>2.5 μM
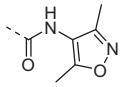	**66**	3000	1500
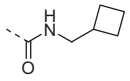	**67**	410	750
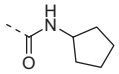	**68**	630	420
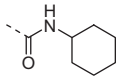	**69**	57	280
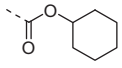	**70**	580	280

Table 6
Exploring the SAR in an effort to affect the serum shift

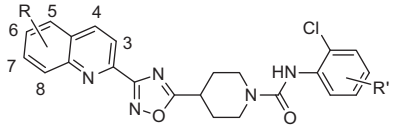

R	R'	Compound	SmoBind 2% FBS IC_{50}(nM)	SmoBind 20% NHS IC_{50}(nM)
H	H	**6**	380	3500
H	4-SO_2Me	**71**	1500	4100
H	5-SO_2Me	**72**	1200	>2.5 μM
H	5-CN	**73**	320	>2.5 μM
H	4-CN	**74**	1900	
3-MeO	H	**75**	>2.5 μM	>2.5 μM
4-MeO	H	**76**	>2.5 μM	>2.5 μM
5-MeO	H	**77**	>2.5 μM	>2.5 μM
6-MeO	H	**78**	1800	
7-MeO	H	**79**	>2.5 μM	>2.5 μM
8-MeO	H	**80**	>2.5 μM	

minimal serum shift, and **87** showed essentially no turn over in rat liver microsomes (Cl_{int} = 8 μL/min/mgP) and in rats the compound showed modest clearance Cl = 40 mL/min/kg and a terminal half life of 0.9 h. Analysis of the urine showed that the parent was the only species excreted.

Introduction of the cyclohexyl or thiopyran dioxide fragments into the benzimidazole core resulted in compounds with similar in vitro properties to the corresponding quinolines **69** and **87**, and both benzimidazoles (**89** and **90**) displayed around one micromolar affinity in the Smo binding assay in the presence of 20% NHS, IC_{50} = 1.1 and 0.76 μM respectively. Similarly to the quinoline series, the cyclohexyl derivative in the benzimidazole series (**89**) displayed high turnover in rat microsomes (Cl_{int} = 192 μL/min/mgP) and relatively high plasma protein binding (rat f_u = 2%). In rats the compound displayed moderate clearance (Cl = 26 mL/min/kg), $T_{1/2}$ = 1.3 h and good oral bioavailability (F = 59%).

A substantial leap in potency was seen with the replacement of the piperidinyl central ring by the corresponding piperazine, and unlike the quinoline system where a 3-fold gain in potency was observed going from **6** to **19**, at least a 20-fold improvement

Table 7
Combining the optimal substituents

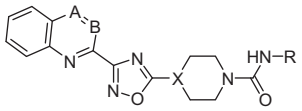

A-B	X		Compound	Light2 IC_{50} (nM)	Smo Bind 2% FBS IC_{50} (nM)	Smo Bind 20% NHS IC_{50} (nM)
CH=CH	CH		**69**	57	280	1600
CH=CH	CH	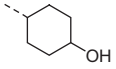	**81**	2700	2500	65% inh. at 25 μM
CH=CH	CH		**82**	480	1700	8600
CH=CH	CHs		**83**	2500	2900	3700
CH=CH	CH	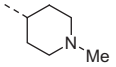	**84**	3200	3400	
CH=CH	CH	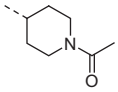	**85**	500	2300	1300
CH=CH	CH	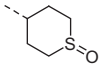	**86**	850	1800	4800
CH=CH	CH	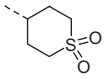	**87**	360	860	1600
CH=CH	CH	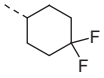	**88**		480	1500
NMe	CH		**89**	89	350	1100
NMe	CH	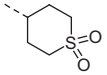	**90**	350	690	760
NMe	N		**91**	5	3	33
NMe	N	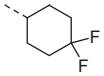	**92**		7	25
CH=CH	N		**93**	53	45	180
CH=CH	N	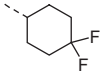	**94**	5	13	39

in potency with the benzimidazoles **89** and **91**. The simple cyclohexyl urea improved in the light2 assay which was run in the presence of minimal serum from 89 nM for **89** to 5 nM for **91**. The addition of the piperazine also had a beneficial effect in reducing the lipophilicity (log *D* = 2.57) of that scaffold, which resulted in a leap in activity from 1.1 μM to 33 nM when this pair of compounds was tested in the Smo binding assay in 20% NHS. This piperazine scaffold also showed modestly improved stability in rat microsomes (Cl_{int} = 119 μL/min/mgP), but in vivo in rats no dramatic change was seen (Cl = 26 mL/min/kg) and due to poor solubility of this particular compound the oral bioavailability was low (*F* = 10%).

The combination of the piperazine and the 2-quinoline yielded some very interesting derivatives suitable for further characterisation, with excellent levels of potency, low serum shift and favourable PK parameters in preclinical species. The simple cyclohexyl (**93**) showed 5-fold improved potency in the Smo binding assay in the presence of 2% FBS (IC_{50} = 45 nM) compared to **69**, and the lower log *D* = 2.76 resulted in only a 4-fold serum shift with IC_{50} = 180 nM in 20% NHS, one of the most potent compounds identified in this series. Room for improvement remained with the pharmacokinetics as this oxadiazole displayed relatively high turnover in liver microsomes (Cl_{int}: rat = 189, dog = 54 and human = 60 μL/min/mgP), and moderate-high clearance in rats (Cl = 54 mL/min/kg) with $T_{1/2}$ = 1.1 h and modest oral bioavailability (F = 24%). In dogs moderate clearance was observed (Cl = 16 mL/min/kg) and $T_{1/2}$ = 1.4 h. The corresponding 4,4'-difluorocyclohexyl (**94**) displayed improved activity with IC_{50} = 5 nM in the light 2 assay, and similar activity in the Smo binding assay in low serum IC_{50} = 13 nM. Similar to the unsubstituted cyclohexyl (**93**), this compound showed only a 3-fold serum shift with IC_{50} = 39 nM in 20% NHS (log *D* = 2.67). The addition of the two fluorine atoms on the cyclohexyl ring stabilised the molecule to oxidative metabolism and it displayed improved stability in microsomes (Cl_{int}: rat = 61, and human = 8 μL/min/mgP). This corresponded to

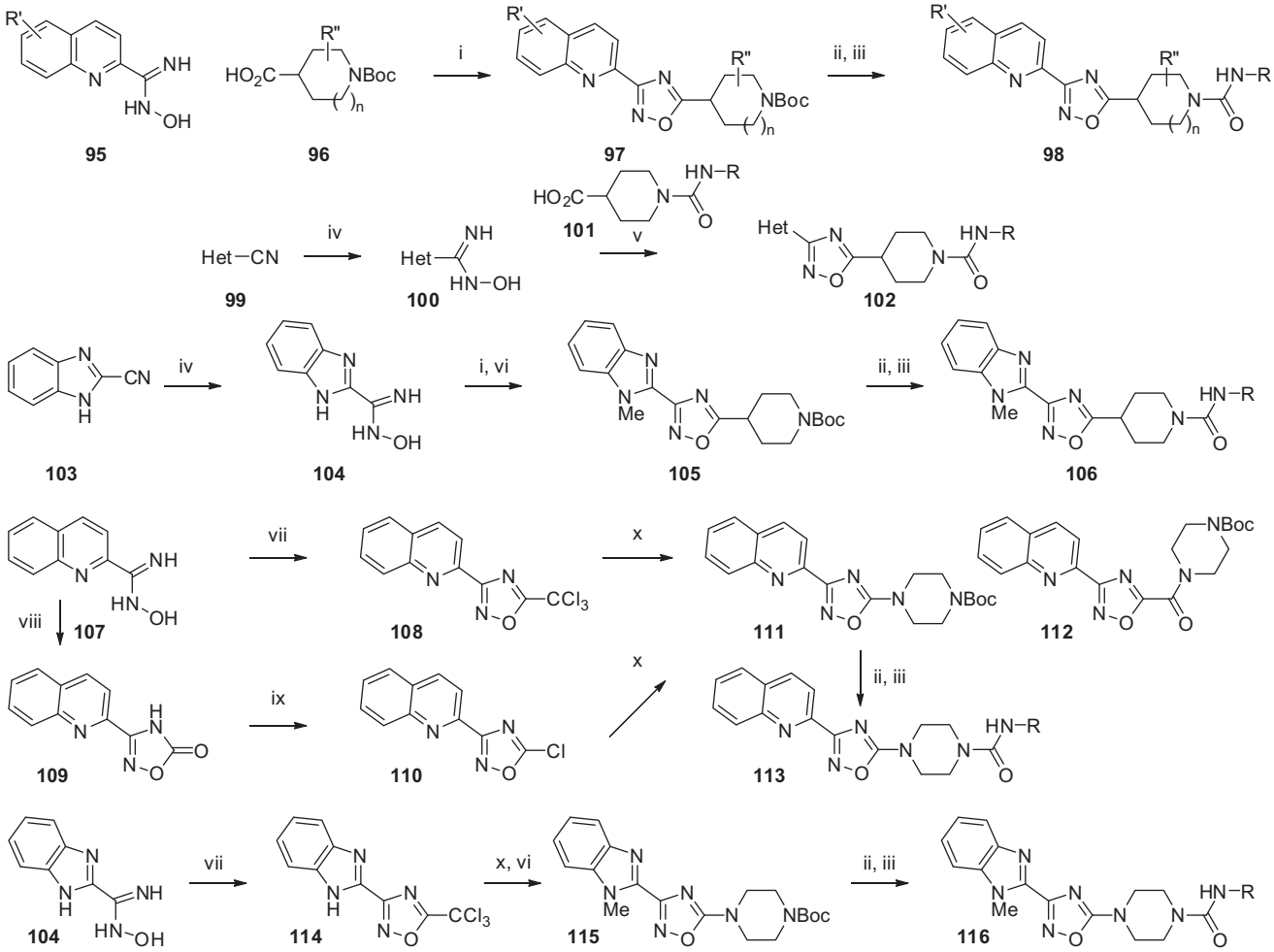

Scheme 1. Synthetic procedure for the preparation of Smo antagonists. Reagents and conditions: (i) 1.2 equiv CDI, DMF, RT, then 1.1 equiv CDI, toluene, Δ, 12 h; (ii) TFA/DCM; (iii) RCNO, DIPEA, DCE/THF or R-NH_2, CDI, MeCN 50 °C or Triphosgene, DIPEA, DCM, −20 °C then R-NH_2; (iv) H_2NOH, $NaHCO_3$, MeOH, Δ; (v) TBTU, Et_3N, DCM, then TBAF, THF; (vi) MeI, KOH, acetone; (vii) Cl_3CCOCl, Cl_3CCO_2H, Δ, 12 h; (viii) CDI, MeCN, Δ, 4 h; (ix) Neat $POCl_3$, 190 °C, uW, 1 hr; (x) Boc-piperazine, DIPEA, THF.

improved clearance in rats (Cl = 32 mL/min/kg) and $T_{1/2}$ = 1.3 h. In dogs moderate clearance was observed (Cl = 20 mL/min/kg) and $T_{1/2}$ = 1.1 h. The addition of the piperazine moiety also improved the off-targets profile as neither compound displayed CYP inhibitor or induction at 30 μM, and IC_{50} >30 μM in hERG binding assays.

These compounds were prepared as outlined in Scheme 1,[16] quinoline-2-yl amidoximes were condensed with various heterocyclic carboxylic acids, and then cyclised to form the required 1,2,4-oxadiazoles **97** using CDI in refluxing toluene. Deprotection and urea formation then furnished the desired Smo antagonists (**98**). Similar chemistry could be applied for the formation of 1,2,4-oxadiazoles (**102**) bearing various aromatic heterocycles at the 3-position, in this case coupling of the piperidine carboxylic acid with the heterocyclic amidoxime was followed up cyclodehydration using TBAF as described by Gangloff.[17] Structural modification to allow introduction of the central piperazine required alternative chemistry, and accordingly *N*-hydroxyquinoline-2-carboximidamide (**107**) was reacted with trichloroacetyl chloride to form the 5-trichloromethyloxadiazole (**108**), although displacement with *N*-Boc piperazine successfully yielded the desired piperazine derivative (**111**) the reaction was complicated by formation of piperazine amide **112** resulting from partial hydrolysis of **108**. Alternatively, the oxadiazol-5(4*H*)-one (**109**) could be prepared and reaction with neat $POCl_3$ in the microwave to give the 5-chlorooxadiazole (**110**) in modest 30% yield. In this case chloride displacement proceeded smoothly enabling the required final compounds (**113**) to be prepared. Similar chemistry was used to synthesize the corresponding benzimidazoles (**116**), although in this case the displacement of the trichloromethyl group in **114** proceeded uneventfully.

In summary, a novel series of weak Smo antagonists were identified through uHTS screening, while these compounds are a novel class of Smo antagonists other ureido derivatives have been described as Smo antagonists.[18–20] Thorough SAR exploration of the scaffold identified the key functionalities necessary for potency, enabling potent nanomolar Smo antagonists like **91** and **94** to be identified. Optimisation of lipophilicity resulted in the most advanced compounds displaying low serum shift and clean off-targets profile, while reduction of intrinsic clearance in liver microsomes resulted in **94** showing moderate clearance in both rats and dogs. These compounds are valuable tools with which to further probe the biology of the Hh-pathway.

Acknowledgments

The authors are extremely grateful to F. Fiore, M. Fonsi, E. Monteagudo, and M. V. Orsale for performing pharmacokinetic studies.

References and notes

1. Rubin, L. L.; de Sauvage, F. J. *Nat. Rev. Drug Disc.* **2006**, *5*, 1026.
2. Xie, J. *Curr. Oncol. Rep.* **2008**, *10*, 107.
3. Gallinari, P.; Filocamo, G.; Jones, P.; Pazzaglia, S.; Steinkuhler, C. *Exp. Opin. Drug Discov.* **2009**, *4*, 525.
4. Ingham, P. W.; McMahon, A. P. *Genes Dev.* **2001**, *15*, 3059.
5. Peukert, S.; Miller-Moslin, K. *ChemMedChem* **2010**, *5*, 500.
6. Robarge, K. D.; Brunton, S. A.; Castanedo, G. M.; Cui, Y.; Dina, M. S.; Goldsmith, R.; Gould, S. E.; Guichert, O.; Gunzner, J. L.; Halladay, J.; Jia, W.; Khojasteh, C.; Koehler, M. F. T.; Kotkow, K.; La, H.; LaLonde, R. L.; Lau, K.; Lee, L.; Marshall, D.; Marsters, J. C.; Murray, L. J.; Qian, C.; Rubin, L. L.; Salphati, L.; Stanley, M. S.; Stibbard, J. H. A.; Sutherlin, D. P.; Ubhayaker, S.; Wang, S.; Wong, S.; Xie, M. *Bioorg. Med. Chem. Lett.* **2009**, *19*, 5576.
7. Von Hoff, D. D.; LoRusso, P. M.; Rudin, C. M.; Reddy, J. C.; Yauch, R. L.; Tibes, R.; Weiss, G. J.; Borad, M. J.; Hann, C. L.; Brahmer, J. R.; Mackey, H. M.; Lum, B. L.; Darbonne, W. C.; Marsters, J. C., Jr.; de Sauvage, F. J.; Low, J. A. *New Eng. J. Med.* **2009**, *361*, 1164.
8. Malancona, S.; Altamura, S.; Filocamo, G.; Kinzel, O.; Martin Hernando, J. I.; Rowley, M.; Scarpelli, R.; Steinkühler, C.; Jones, P. *Bioorg. Med. Chem. Lett.* **2011**. doi:10.1016/j.bmcl.2011.06.024.
9. Kinzel, O.; Alfieri, A.; Altamura, S.; Brunetti, M.; Bufali, S.; Colaceci, F.; Ferrigno, F.; Filocamo, G.; Fonsi, M.; Gallinari, P.; Malancona, S.; Martin Hernando, J. I.; Monteagudo, E.; Orsale, M. V.; Palumbi, M. C.; Pucci, V.; Rowley, M.; Sasso, R.; Scarpelli, R.; Steinkühler, C.; Jones, P. *Bioorg. Med. Chem. Lett.* **2011**. doi:10.1016/j.bmcl.2011.06.023.
10. Stanton, B. Z.; Peng, L. F.; Maloof, N.; Nakai, K.; Wang, X.; Duffner, J. L.; Taveras, K. M.; Hyman, J. M.; Lee, S. W.; Koehler, A. N.; Chen, J. K.; Fox, J. L.; Mandinova, A.; Schreiber, S. L. *Nature Chem. Biol.* **2009**, *5*, 154.
11. Lauth, M.; Bergström, A.; Shimokawa, T.; Toftgård, R. *Proc. Natl. Acad. Sci. U.S.A.* **2007**, *104*, 8455.
12. Hyman, J. M.; Firestone, A. J.; Heine, V. M.; Zhao, Y.; Ocasio, C. A.; Han, K.; Sun, M.; Rack, P. G.; Sinha, S.; Wu, J. J.; Solow-Cordero, D. E.; Jiang, J.; Rowitch, D. H.; Chen, J. K. *Proc. Natl. Acad. Sci. U.S.A.* **2009**, *106*, 14132.
13. Rifai, Y.; Arai, M. A.; Sadhu, S. K.; Ahmed, F.; Ishibashi, M. *Bioorg. Med. Chem. Lett.* **2011**, *21*, 718.
14. Taipale, J.; Chen, J. K.; Cooper, M. K.; Wang, B.; Mann, R. K.; Milenkovic, L.; Scotts, M. P.; Beachy, P. A. *Nature* **2000**, *406*, 1005; Frank-Kamenetsky, M.; Zhang, X. M.; Bottega, S.; Guicherit, O.; Wichterle, H.; Dudek, H.; Bumcrot, D.; Wang, F. Y.; Jones, S.; Shulok, J.; Rubin, L. L.; Porter, J. A. *J. Biol.* **2002**, *1*, 10.
15. Chen, J. K.; Taipale, J.; Cooper, M. K.; Beachy, P. A. *Genes Dev.* **2002**, *16*, 2743.
16. Dessole, G.; Jones, P.; Llauger Bufi, L.; Muraglia, E.; Ontoria Ontoria, J. M.; Torrisi, C. WO2010/013037, 2010.
17. Gangloff, A. R.; Litvak, J.; Shelton, E. J.; Sperandio, D.; Wang, V. R.; Rice, K. D. *Tetrahedron Lett.* **2001**, *42*, 1441.
18. Brunton, S. A.; Stibbard, J. H. A.; Rubin, L. L.; Kruse, L. I.; Guicherit, O. M.; Boyd, E. A.; Price, S. *J. Med. Chem.* **2008**, *51*, 1108.
19. Manetti, F.; Faure, H.; Roudaut, H.; Gorojankina, T.; Traiffort, E.; Schoenfelder, A.; Mann, A.; Solinas, A.; Taddei, M.; Ruat, M. *Mol. Pharmacol.* **2010**, *78*, 658.
20. Roudaut, H.; Traiffort, E.; Gorojankina, T.; Vincent, L.; Faure, H.; Schoenfelder, A.; Mann, A.; Manetti, F.; Solinas, A.; Taddei, M.; Ruat, M. *Mol. Pharmacol* **2011**, *79*, 453.